Intrachain Triplet Energy Transfer in Platinum−Acetylide Copolymers

Kirk S. Schanze,* Eric E. Silverman, and Xiaoming Zhao

Department of Chemistry, University of Florida, Gainesville, Florida 32611-7200

Received: May 27, 2005; In Final Form: July 22, 2005

A series of platinum−acetylide homo- and copolymers was prepared and characterized by using photophysical methods. The polymers feature repeat units of the type [*trans*-Pt(PBu_3)$_2$(−C≡C−Ar−C≡C−)], where Ar = 1,4-phenylene (P) or 2,5-thienylene (T). The properties of homopolymers that contain only the 1,4-phenylene or 2,5-thienylene repeat units were compared with those of random copolymers having the structure −[−(Pt(PBu_3)$_2$(−C≡C−T−C≡C−))$_x$−(Pt(PBu_3)$_2$(−C≡C−P−C≡C−))$_{(1-x)-}$] where x = 0.05, 0.15, and 0.25. Absorption and photoluminescence spectroscopy demonstrates that the singlet and triplet excitations localized on 1,4-phenylene units are higher in energy relative to those localized on the 2,5-thienylene units. The mechanism and dynamics of intrachain triplet energy transfer from 1,4-phenylene to the 2,5-thienylene repeats were explored in the copolymers. Photoluminescence and nanosecond transient absorption spectroscopy indicate that at room temperature P → T energy transfer is efficient and rapid ($k \gg 10^8$ s^{-1}), even in the copolymer that contains only 5% 2,5-thienylene repeat units. At 77 K, steady-state and time-resolved photoluminescence spectroscopy reveals that triplet energy transfer is much less efficient and a fraction of the triplet excitations is "trapped" on the high-energy 1,4-phenylene units. Intrachain energy transfer is believed to occur by two mechanisms, one involving P → T singlet energy transfer followed by intersystem crossing, whereas the other involves intersystem crossing prior to P → T triplet energy transfer. The relationship between the observed energy transfer efficiencies and mechanisms in the copolymers is discussed.

Introduction

Conjugated polymers have attracted a great deal of attention over the past several decades.[1,2] Interest in this field is motivated by the variety of applications that exist for conjugated polymers as the active components in electronic, electrooptical, and optical devices.[2] Platinum−acetylide-based conjugated polymers have attracted interest because their photophysical properties are dominated by long-lived, phosphorescent $^3\pi,\pi^*$ excited states.[3−9] This feature allows the facile study of the properties of the triplet state in conjugated electronic systems. In addition, because of their high triplet yield and relatively large triplet−singlet radiative decay rates, platinum−acetylide polymers are of interest for use in electrophosphorescent devices[10,11] and as the active material in nonlinear optical applications.[12]

To better understand the properties of conjugated polymers, several groups have investigated the relationship between polymer structure and transport of excitons and charged carriers.[5,13−21] These investigations, for the most part, have examined exciton and charge carrier transport in the solid state by using electronic and optical techniques. However, for some applications, especially in molecular electronics, it is envisioned that conjugated materials will not be used as solids but rather as isolated single chain "molecular wires".[22] Consequently, recent work has focused on the study of intrachain carrier transport in conjugated polymers.[23−31] The most common technique used to investigate intrachain transport is the use of dilute solutions where polymer aggregation and interchain interactions are minimized.[32] To date, most investigations have focused on the study of intrachain transport of positive polarons (holes) and singlet excitons.[23,27,31−35]

Despite these efforts, relatively little is known about intrachain transport of triplet excitons in conjugated polymers.[36] We therefore initiated an investigation of triplet exciton transport in a series of platinum−acetylide copolymers. The primary objectives of this work are to study the efficiency and dynamics of intrachain triplet exciton transfer in platinum−acetylide polymer chains. The structures of the polymers used for this study are shown in Chart 1. Platinum acetylides were chosen because their triplet states are phosphorescent and thus easily monitored by photoluminescence spectroscopy.[3−7] Furthermore, these polymers are synthesized relatively easily using CuI-catalyzed Hagihara coupling of platinum(II) chlorides with terminal acetylenes.[37] To study triplet exciton transfer in these materials, a series of copolymers was prepared that contain randomly distributed 2,5-thienylene repeats within a polymer consisting primarily of 1,4-phenylene repeat units. In the copolymers, the 2,5-thienylene unit functions as a "trap" for triplet excitons. This is because the energy of the triplet state localized on a Pt−C≡C−T−C≡C−Pt chromophore (Pt−T) lies 0.3−0.4 eV lower than the triplet localized on the Pt−C≡C−P−C≡C−Pt chromophore (Pt−P).[4,38,39] A series of copolymers that contain various loadings of the 2,5-thienylene trap was

CHART 1

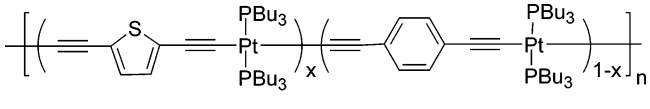

Homopolymers		Copolymers	
P_{100}	: x = 0	$P_{95}T_5$	: x = 0.05
T_{100}	: x = 1	$P_{85}T_{15}$	: x = 0.15
		$P_{75}T_{25}$	: x = 0.25

* To whom correspondence should be addressed. Tel: 352-392-9133. Fax: 352-392-2395. E-mail: kschanze@chem.ufl.edu. Website: http://www.chem.ufl.edu/~kschanze.

10.1021/jp052818i CCC: $30.25
Published on Web 09/08/2005

investigated to explore the effect of distance on the efficiency of triplet exciton transfer.

In the present manuscript we provide a complete report on the synthesis and photophysical characterization of the Pt−acetylide copolymers. The results indicate that at ambient temperature intrachain triplet exciton transfer is rapid ($k \geq 10^8$ s^{-1}). However, at low temperature (77 K) long distance triplet transfer is slowed such that exciton transfer dynamics are observed on the microsecond time scale, suggesting that the rate of triplet hopping is significantly slower than that at ambient temperature.

Experimental Section

General Synthesis and Materials. *trans*-Bis(tributylphosphine)palladium dichloride ($Pd(PPh_3)_2Cl_2$) and tetrakis(tributylphosphine)palladium were purchased from Strem Chemicals and used as received. Tetrahydrofuran and 2-methyltetrahydrofuran (THF and 2-MTHF) were purchased from Acros and distilled from sodium/benzophenone under argon before use. All other reagents and solvents were purchased from either Acros or Aldrich and used as received unless otherwise noted. ^1H, ^{13}C, and ^{31}P NMR spectra were recorded on a Varian 300 MHz spectrometer. Column chromatography was performed using silica gel (Merk, 230−400 mesh). Gel permeation chromatography (GPC) was done on a Rainin Dynamax model SD-200 solvent delivery system equipped with two PL-Gel 5 Mixed D columns (Polymer Laboratories, Inc., Amherst, MA) and a UV detector set at a wavelength where the polymer under investigation was known to absorb. Polymer molecular weight information was calculated using Polymer Laboratories software and is reported relative to polystyrene standards. The synthesis and characterization of 1,4-diethynylbenzene and P_{100} have been described previously.[31,40]

Photophysical Methods. UV−vis absorption spectra were obtained with samples contained in 1 cm quartz cuvettes using a Varian Cary 100 spectrophotometer. Corrected, steady-state photoluminescence spectra were recorded on a SPEX F-112 fluorescence spectrophotometer. Samples were contained in 1 cm × 1 cm quartz cuvettes, and the optical density was adjusted to approximately 0.1 at the excitation wavelength. All photophysical measurements were carried out in argon degassed THF solutions except for those conducted at 77 K, which were carried out in argon degassed 2-MTHF. Emission quantum yields are reported relative to $Ru(bpy)_3$ in water for which $\Phi = 0.055$,[41] and an appropriate correction was applied for the difference in refractive indices of actinometer and sample solvent.[42] Nanosecond−microsecond time-resolved absorption and emission spectroscopy were carried out by using methods and instrumentation that have been previously described.[40,43]

2,5-Diiodothiophene (1). To a flask containing a mixture of acetic acid and chloroform (14 mL, 3:4) was added thiophene (1.00 g, 11.9 mmol) and *N*-iodosuccinimide (5.84 g, 24.4 mmol). The flask was covered, and the mixture was stirred at room temperature for 16 h. The reaction mixture was then washed with an aqueous solution of sodium thiosulfate (10%) and pure water. The organic phase was dried over $MgSO_4$, and the solvent was removed under reduced pressure. Column chromatography with hexanes afforded the desired product as a reddish solid, yield 2.80 g (70%). ^1H NMR ($CDCl_3$, 300 MHz) δ 6.90 (s, 2H); ^{13}C NMR ($CDCl_3$, 300 MHz) δ 76.36, 138.65.

2,5-Bis(trimethylsilylethynyl)thiophene (2). To a flask charged with 8 mL of a 1:1 (v:v) mixture of THF and diiospropylamine was added to 2,5-diodothiophene (668 mg, 2.0 mmol). The resulting solution was degassed for 30 min by purging with argon. Trimethylsilylacetylene (491 mg, 5 mmol), $Pd(PPh_3)_4$ (12 mg, 1.6 mmol), and copper iodide (4 mg, 2 mmol) were added to this solution. The reaction was then stirred at room temperature for 24 h. After this time, the solvent was removed under reduced pressure. Flash chromatography of the residue with hexanes gave the desired product as a yellow solid, yield 440 mg (80%). ^1H NMR ($CDCl_3$, 300 MHz) δ 0.24 (s, 18H), 7.04 (s, 2H); ^{13}C NMR ($CDCl_3$) δ −0.23, 96.86, 99.90, 124.47, 132.29.

Compound 3. CuI (3 mg) and tetrabutylammonium fluoride (0.51 mL of a 1 M solution in THF, 0.51 mmol) were added to a flask charged with $Pt(PBu_3)_2Cl_2$ (501 mg, 0.75 mmol) and **2** (69 mg, 0.25 mmol) in a 3:1 (v:v) mixture of toluene and piperidine (12 mL). The reaction mixture was deoxygenated by purging with argon for 15 min. After the reaction mixture was stirred for 2 days at room temperature, the solvent was removed under reduced pressure. The residue was stirred in dichloromethane, and the resulting suspension was filtered. The soluble portion was collected and purifed by flash chromatography with hexanes as the eluent to afford **3** as a yellow solid, yield 224 mg (64%). ^1H NMR ($CDCl_3$) δ 0.93 (t, $J = 7.20$ Hz, 36H), 1.38−1.62 (m, 48H), 1.90−2.00 (m, 24H), 6.61 (s, 2H); ^{13}C NMR ($CDCl_3$) δ 13.76, 21.90 (t, $J = 66.30$ Hz), 24.24 (t, $J = 27.9$ Hz), 26.01, 88.26, 93.77, 126.84; ^{31}P NMR ($CDCl_3$, 121 MHz) δ 8.04 (d, $J_{Pt-P} = 2360$ Hz).

$P_{95}T_5$. An ampule charged with 3 mL of a 1:5 (v:v) mixture of diisopropylamine and toluene with a small magnetic stirring bar was fitted with a septum and purged with argon for 5 min. The ampule was then subjected to reduced pressure for 1 min by inserting a needle connected by hoses to a water aspirator into the septum. This process was repeated twice, ending with argon purging. To the ampule were rapidly added **3** (14 mg, 0.01 mmol), 1,4-diethynylbenzene (24 mg, 0.19 mmol), CuI (2 mg, 0.01 mmol), and $Pd(PPh_3)_4$ (120 mg, 0.18 mmol). The solution was degassed by three more argon−vacuum cycles, sealed under vacuum, and stirred at room temperature for 24 h. After this time, the ampule was broken and the solution was poured into 50 mL of methanol to induce precipitation of the polymer as a yellow solid. The yellow precipitate was collected by filtration and washed with methanol and then water. This solid was dissolved in a minimal amount of chloroform, precipitated again into methanol, and collected by filtration to yield the desired polymer as a yellow solid, yield 96 mg (70%). ^1H NMR (300 MHz, $CDCl_3$) δ 0.77−1.03 (br, 72H), 1.30−1.72 (br, 96H), 1.86−2.25 (br, 48H), 6.57−6.61 (s, 0.48H), 7.03−7.11 (d, 3.15H), 7.14−7.32 (m, 11.19H). GPC: $M_n = 4570$; $M_w = 12\,800$; PDI = 2.81.

$P_{85}T_{15}$. This copolymer was prepared according to the same procedure used for **$P_{95}T_5$** except the reagents used were as follows: **3** (47 mg, 0.03 mmol), $Pt(PBu_3)_2Cl_2$ (105 mg, 0.16 mmol), 1,4-diethynylbenzene (24 mg, 0.19 mmol), and CuI (2 mg, 0.01 mmol). $P_{85}T_{15}$ was obtained as a yellow solid, yield 99 mg (72%). ^1H NMR (300 MHz, $CDCl_3$) δ 0.76−1.02 (m, 72H), 1.32−1.75 (m, 96H), 1.84−2.25 (m, 48H), 6.58−6.61 (s, 0.67H), 7.04−7.12 (m, 2.53H), 7.18−7.27 (m, 6.22H). GPC: $M_n = 3370$; $M_w = 11\,800$; PDI = 3.51.

$P_{75}T_{25}$. This copolymer was prepared according to the same procedure used for $P_{95}T_5$ except the amounts of reagents used were as follows: **3** (70 mg, 0.05 mmol), $Pt(PBu_3)_2Cl_2$ (67 mg, 0.10 mmol), 1,4-diethynylbenzene (18 mg, 0.15 mmol), and CuI (2 mg, 0.01 mmol). $P_{75}T_{25}$ was obtained as a yellow solid, yield 85 mg (78%). ^1H NMR (300 MHz, $CDCl_3$) δ 0.81−1.04 (m, 72H), 1.32−1.74 (m, 96H), 1.85−2.24 (m, 48H), 6.58−6.02

SCHEME 1[a]

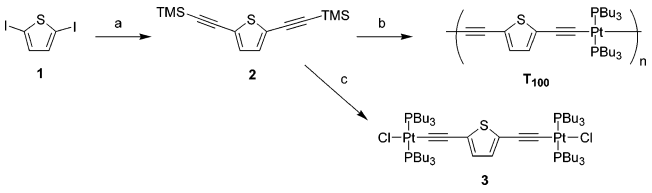

[a] Reagents and Conditions: (a) $Pd(PPh_3)_4$, CuI, trimethylsilylacetylene; (b) $Pt(PBu_3)_2Cl_2$ (1 equiv), Bu_4NF, toluene/piperidine; (c) $Pt(PBu_3)_2Cl_2$ (3.5 equiv), Bu_4NF, toluene/piperidine.

(s, 1.53H), 7.04−7.15 (br, 7.22H), 7.18−7.29 (m, 4.96H). GPC: $M_n = 28\,900$; $M_w = 106\,000$; PDI = 3.67.

T_{100}. This polymer was prepared according to the same procedure used for $P_{95}T_5$ except the amounts of reagents used were as follows: **3** (69 mg, 0.25 mmol), $Pt(PBu_3)_2Cl_2$ (167 mg, 0.25 mmol), tetrabutylammonium fluoride (0.51 mL of a 1 M solution in THF), and CuI (1 mg, 0.005 mmol). T_{100} was obtained as a yellow solid, yield 145 mg (80%). ^{1}H NMR (300 MHz, $CDCl_3$) δ 0.09 (m, 18 H), 1.50 (m, 27 H), 2.1 (br 12 H), 6.48 (s, 2H). GPC: $M_n = 39\,100$; $M_w = 81\,200$; PDI = 2.08.

Results and Discussion

Polymer and Copolymer Synthesis and Structure. The chemical structures of the polymers that are the focus of this work are presented in Chart 1. The nomenclature adopted for the copolymers is P_xT_y where x and y are the mole fractions (expressed as percentages) of phenylene and thienylene monomers, respectively, used in the polymerizations.

It was originally envisioned that these polymers would be prepared by CuI-catalyzed coupling of appropriate amounts of 2,5-diethynylthiophene, 1,4-diethynylbenzene, and $Pt(PBu_3)_2Cl_2$. Unfortunately, 2,5-diethynylthiophene is unstable under the conditions used for the polymerization reactions. However, since 2,5-bis(trimethylsilylethynyl)thiophene is quite stable under the polymerization conditions, it was deprotected in situ with tetrabutylammonium fluoride under the Hagiara conditions with 1 equiv of $Pt(PBu_3)_2Cl_2$ to afford T_{100} (Scheme 1).

The synthesis of the copolymers $P_{95}T_5$, $P_{85}T_{15}$, and $P_{75}T_{25}$ proved to be more challenging, as in situ deprotection of **2** under Hagihara conditions with an appropriate amount of 1,4-diethynylbenzene and $Pt(PBu_3)_2Cl_2$ yielded only low molecular weight oligomers. In previous work, 1,4-diethynylbenzene was diplatinated with excess $Pt(PBu_3)_2Cl_2$, and the resulting Pt−acetylide dimer, featuring monochlorinated platinum end groups, was used in further Hagihara coupling reactions.[9] Extending this methodology to a thiophene-based monomer, **2** was deprotected in situ with tetrabutylammonium fluoride in the presence of CuI and an excess of $Pt(PBu_3)_2Cl_2$ to afford dimer **3** (Scheme 1). Subsequent polymerization of **3** in a three component A−A + A′−A′ + B−B polymerization with appropriate amounts of 1,4-diethynylbenzene, $Pt(PBu_3)_2Cl_2$, and CuI affords copolymers $P_{95}T_5$, $P_{85}T_{15}$, and $P_{75}T_{25}$, as shown in Scheme 2.

These copolymers feature a platinum−acetylide backbone in which 1,4-phenylene is the predominant repeat unit, and the 2,5-thienylene repeat is incorporated at various loadings. This synthetic design, wherein the thiophene repeat unit is introduced via dimer **3**, has an advantage in that it prevents the formation of "blocks" of adjacent thiophene-containing repeat units in the copolymer. This is because dimer **3** can only react with 1,4-diethynylbenzene under the Hagihara reaction conditions.

The aromatic region of the ^{1}H NMR spectra of the platinum−acetylide copolymers is particularly useful in helping to elucidate the structure and composition of the materials (Figure 1). First, the P_{100} and T_{100} homopolymers (parts a and e of Figure 1, respectively) exhibit aromatic resonances at $\delta \approx 7.2$ and 6.6 ppm, respectively, arising from the protons on the phenylene and thienylene rings (blue and red dots in Figure 1). Interestingly, the copolymers feature resonances at approximately the same positions; however, each copolymer exhibits an additional resonance at $\delta \approx 7.1$ ppm (green dots in parts b−d of Figure 1). The structure at the top of Figure 1 provides assignments for the resonances in the copolymers. To understand these assignments, it is important to recognize that there are two "types" of phenylene units in the copolymers: (1) phenylenes that are adjacent to other phenylenes (blue dots in the structure) and (2) phenylenes that are adjacent to a thienylene unit (green dots in the structure). We believe that the new peak that appears at 7.1 ppm in the copolymers arises from phenylenes that are adjacent to a thienylene unit (green dots in the structure). Note that the amplitude of the 7.1 ppm resonance is larger than that of the 7.2 ppm resonance in $P_{75}T_{25}$. This is in accord with the fact that in this copolymer on average there is one thienylene in every four Pt−acetylide repeats; therefore on average two out of three phenylenes are adjacent to a thienylene. This observation has important implications—the NMR spectra give clear evidence that in the ground state the electronic interaction between adjacent phenylene and thienylene units is sufficiently strong to give rise to a 0.1 ppm upfield shift in the chemical shift of the phenylene protons. Given the significant ground-state interaction, then it is reasonable to expect that there will also be interactions between adjacent residues in the excited state as well.

In addition to giving qualitative information concerning structure, the aromatic region of the NMR spectra can be integrated to give quantitative information regarding the loading of thienylene residues in the copolymers. On the basis of the integrations, the ratio of thiophene to phenylene in $P_{95}T_5$, $P_{85}T_{15}$, and $P_{75}T_{25}$ is found to be relatively close to that expected on the basis of the monomer feed used in the polymerization reactions.

Absorption and Photoluminescence Spectroscopy. The UV−vis absorption spectra of the platinum−acetylide polymers and copolymers in THF solution are presented in Figure 2, and Table 1 summarizes the photophysical parameters, including the absorption band maxima. The absorption spectra of the two homopolymers, P_{100} and T_{100}, are shown together in Figure 2a. Both spectra appear as broad bands, with $\lambda_{max} = 341$ and 402 nm, for P_{100} and T_{100}, respectively. In each case, the absorption is due to the long-axis polarized π,π^* transition of the platinum−acetylide backbone. The red shift in the absorption of T_{100} relative to P_{100} reflects a 0.5 eV reduction in the HOMO−LUMO gap for the thiophene-based polymer relative to the phenylene polymer.

SCHEME 2

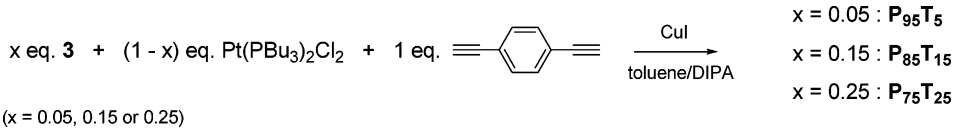

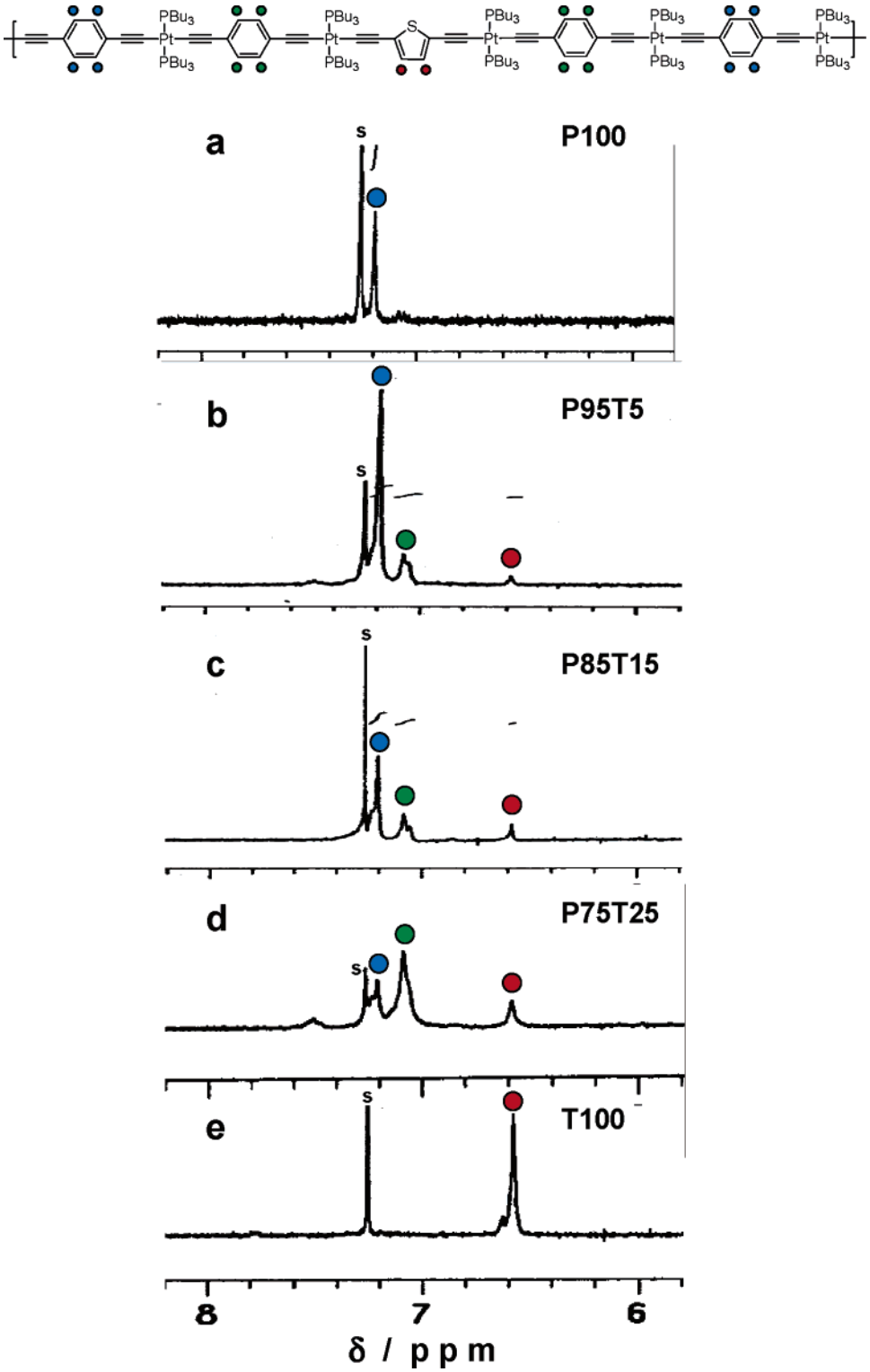

Figure 1. Expansion of the aromatic region of the ^{1}H NMR spectra of polymers used in this study. Structure at top provides spectral assignments (s indicates solvent peak).

The absorption spectra of the copolymers are shown together in Figure 2b. First, the spectrum of $P_{95}T_5$ is dominated by a broad band with $\lambda_{max} = 347$ nm, with a shoulder on the low-energy side at ca. 395 nm. The primary absorption band is very similar in shape and energy compared to that of P_{100}, and on this basis it is assigned to the phenylene-based repeat units (Pt−P) in the Pt−acetylide backbone. The shoulder at 395 nm appeared at a similar wavelength compared to the absorption of the T_{100} homopolymer, and on this basis it assigned to chromophores in the chain that contain the thienylene unit (Pt−T).

The absorption spectrum of $P_{85}T_{15}$ features the same two bands seen in $P_{95}T_5$; however, the relative intensity of the Pt−T (395 nm) shoulder is substantially increased. While this is consistent with the fact that there is an increase in the number of thiophene units in $P_{85}T_{15}$, the relative intensity of the low-energy band is significantly greater than might be expected if the transition arises due solely to the (−Pt−C≡C−T−C≡C−

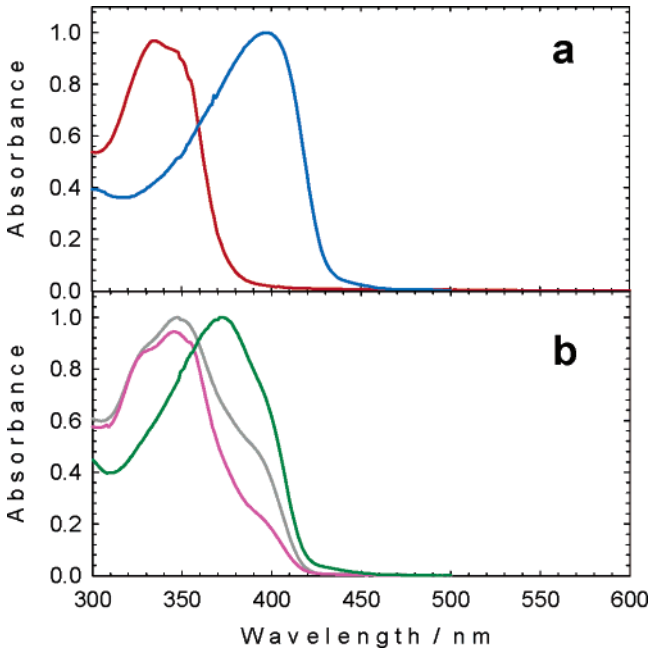

Figure 2. Normalized absorption spectra of polymers in THF solution: (a) P_{100} (red line), T_{100} (blue line); (b) $P_{95}T_5$ (pink line), $P_{85}T_{15}$ (gray line), $P_{75}T_{25}$ (green line).

TABLE 1: Absorption and Emission Properties of Polymers[a]

polymer	absorption λ_{max}/nm	emission[b] λ_{max}^F/nm	λ_{max}^P/nm	$\tau/\mu s$[c]	ϕ^F	ϕ^P
P_{100}	341		514	18		0.045
$P_{95}T_5$	347	420	604	9.1	0.002	0.071
$P_{85}T_{15}$	347	420	604	7.7	0.063	0.058
$P_{75}T_{25}$	375	420	604	7.1	0.053	0.043
T_{100}	402	420	604	5.6	0.057	0.031

[a] Measurements for THF solutions at ambient temperature (argon outgassed for lifetime and quantum yield measurements). [b] F and P superscripts indicate fluorescence and phosphorescence, respectively. ϕ is emission quantum efficiency. [c] Emission lifetime measured at phosphorescence emission maximum (see left adjacent column).

Pt−) repeat unit. Specifically, in $P_{85}T_{15}$ there is on average only one thiophene for every seven repeat units in the polymer chain, yet the relative intensity of the 395 nm absorption shoulder is ca. 50% of that of the main UV band. Thus, we conclude that the thiophene unit influences the absorption of a segment of the platinum−acetylide chain that includes several adjacent phenylene-containing units. This concept is reinforced further by the absorption spectrum of $P_{75}T_{25}$. Interestingly, for this copolymer the primary absorption band is red shifted to 375 nm, and the low-energy transition appears only as an inflection on the low-energy side of the band. Apparently in $P_{75}T_{25}$ there is a sufficiently high loading of thiophene units in the polymer chain such that the absorption of all of the phenylene units is influenced.

Taken together, the absorption spectra of the homo- and copolymers provide an indication of the structure of the chromophore responsible for the allowed radiative transition from the ground state to the singlet excited state. Figure 3 provides a schematic of the situation for $P_{95}T_5$ and $P_{75}T_{25}$, which represent, respectively, low and high thiophene loading in the Pt−acetylide backbones. Our model is that in the Franck−Condon singlet state that is produced by light absorption from the ground state, the initially produced $^1\pi,\pi^*$ exciton is delocalized over a chromophore consisting of at least three aryl residues. In particular, the low-energy optical transition which appears as a shoulder at ca. 395 nm in $P_{95}T_5$ likely is due to a chromophore which is approximated by the region encompassed by the oval in Figure 3a. Because of the considerably higher thiophene loading in $P_{75}T_{25}$, these chromophores essentially "merge" as shown schematically in Figure 3b. In this polymer there are very few phenylene repeat units that are not directly adjacent to a thiophene repeat, and consequently, the primary absorption band is red shifted as seen in Figure 2b. The concept that the singlet exciton is delocalized over three or more repeat units in Pt−acetylides is consistent with our earlier work on monodisperse Pt−acetylide oligomers which showed clear evidence that the Franck−Condon singlet exciton is delocalized over several repeat units in the oligomers.[9]

Photoluminescence spectra were obtained for the homo- and copolymers as solutions in THF at room temperature and in a 2-methyltetrahydrofuran glass at 77 K (Figure 4). The spectra of the homopolymers P_{100} and T_{100} obtained at room temperature are shown in parts a and e of Figure 4, respectively. The luminescence from P_{100} is dominated by a band with λ_{max} = 514 nm which is due to phosphorescence from the $^3\pi,\pi^*$ manifold.[9] The emission from T_{100} features two broad bands with λ_{max} = 420 and 604 nm. The high energy band is due to fluorescence from $^1\pi,\pi^*$, whereas the low energy band is phosphorescence from the $^3\pi,\pi^*$ manifold.[4] The phosphorescence assignment is supported by a lifetime of 5.6 μs. On the basis of the phosphorescence energies for P_{100} and T_{100} (2.41 and 2.05 eV, respectively), it is evident that the energy of the $^3\pi,\pi^*$ state localized on a Pt−T repeat unit is ca. 0.35 eV lower in energy than that localized on a Pt−P repeat. Consequently, in the copolymers, it is anticipated that intrachain triplet energy transfer as shown in eq 1 is exothermic

$$\ldots{}^3[\text{Pt}-\text{P}-\text{Pt}]^*-\text{P}-\text{Pt}-\text{P}-\text{Pt}-\text{P}-\text{Pt}-\text{T}-\text{Pt}\ldots \rightarrow \ldots\text{Pt}-\text{P}-\text{Pt}-\text{P}-\text{Pt}-\text{P}-\text{Pt}-\text{P}-{}^3[\text{Pt}-\text{T}-\text{Pt}]^*\ldots \quad (1)$$

where P = phenylene repeat and T = thienylene repeat.

The photoluminescence spectra of the copolymers are shown in parts b−d of Figure 4; in each case the spectra obtained at 298 and 77 K are shown in red and blue, respectively. The emission spectra were obtained with 350 nm excitation, which corresponds in each case to excitation into the dominant absorption band. For $P_{95}T_5$, the emission at 298 K is dominated by a band with λ_{max} = 604 nm that corresponds to Pt−T phosphorescence. A very weak band is seen at λ = 515 nm, which corresponds to phosphorescence from Pt−P. Interestingly, the spectrum of $P_{95}T_5$ obtained at 77 K is dominated by the Pt−P phosphorescence band at λ = 510 nm, with the Pt−T emission appearing as a relatively weak shoulder at λ = 600 nm (the slight blue shifts in the low-temperature emission are expected due to the rigid solvent environment). The 298 K emission spectra of $P_{85}T_{15}$ and $P_{75}T_{25}$ are similar, with each spectrum featuring Pt−T fluorescence at 420 nm and Pt−T phosphorescence at 604 nm. The 298 K spectrum of $P_{85}T_{15}$ features a very weak peak at 515 nm arising from Pt−P, but this band is absent in $P_{75}T_{25}$. At 77 K the emission spectra of $P_{85}T_{15}$ and $P_{75}T_{25}$ are quite different—the former is dominated by the Pt−P phosphorescence (λ = 510 nm), with a relatively weaker peak at λ = 600 nm which corresponds to Pt−T phosphorescence, whereas the emission of the latter polymer is dominated by the Pt−T phosphorescence at ca. 600 nm.

Qualitatively, the emission data indicates that at room temperature intrachain energy transfer from Pt−P to Pt−T as shown in eq 1 is very efficient in all of the copolymers. This finding is especially interesting in the case of $P_{95}T_5$, which

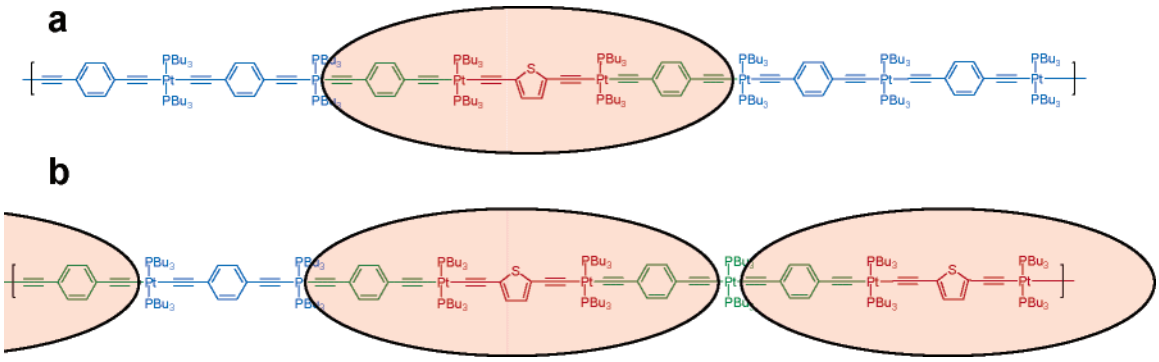

Figure 3. Schematic diagram illustrating possible extent of delocalization of singlet excited state around Pt−T chromophore immediately following light absorption (Franck−Condon singlet state).

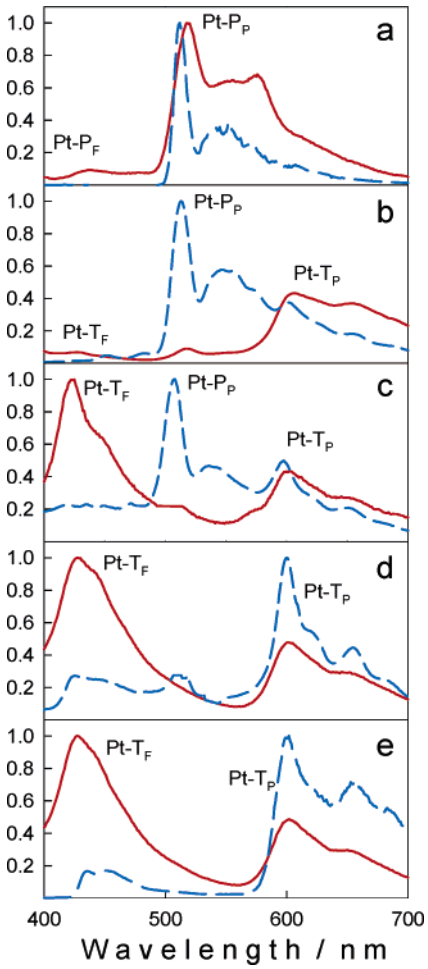

Figure 4. Emission spectra of polymers in degassed solutions: (a) P_{100}, (b) $P_{95}T_5$, (c) $P_{85}T_{15}$, (d) $P_{75}T_{25}$, and (e) T_{100} (solvent: room temperature, THF; 77 K, 2-MTHF, $c \approx 10^{-5}$ M in polymer repeat unit). Solid lines (red), room temperature; dashed lines (blue), 77 K. Subscripts F and P on labels indicate fluorescence and phosphorescence, respectively. Excitation wavelengths: 350 nm for P_{100}, $P_{95}T_5$, $P_{85}T_{15}$, and $P_{75}T_{25}$; 380 nm for T_{100}.

contains on average only 1 Pt−T unit for every 20 polymer repeat units. This result suggests that the process(es) leading to intrachain energy transfer from Pt−P to Pt−T are very rapid at ambient temperature. By contrast, the emission spectra of the copolymers at 77 K indicate that intrachain energy transfer is much less efficient at low temperature. This is especially true for $P_{95}T_5$ and $P_{85}T_{15}$, where the low-temperature emission spectra are dominated by the high-energy emission from Pt−P repeat units. On the other hand, for $P_{75}T_{25}$, energy transfer is efficient, even at low temperature. The mechanisms and

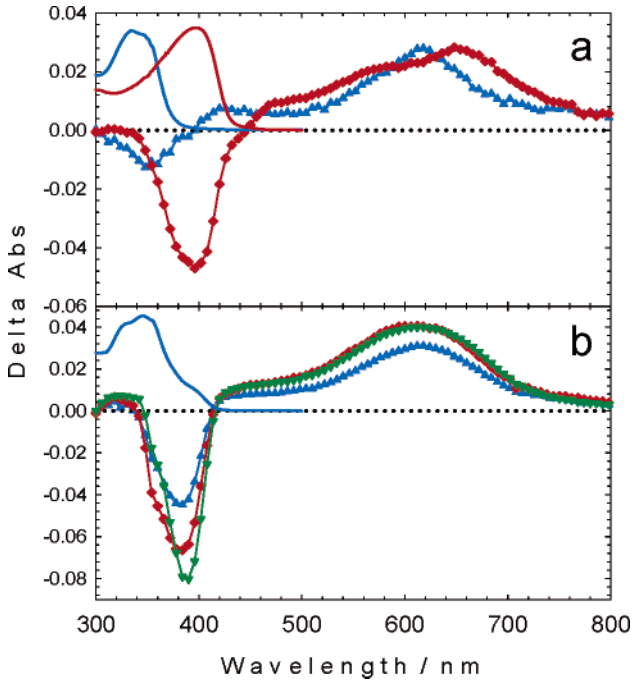

Figure 5. Transient absorption spectra obtained 100 ns after 355 nm excitation (10 nm, 20 mJ cm^{-2}): (a) P_{100} (blue triangle), T_{100} (red diamond), solid lines show ground-state absorption spectra of P_{100} (red line) and T_{100} (blue line); (b) $P_{95}T_5$ (blue triangle), $P_{85}T_{15}$ (red diamond), $P_{75}T_{25}$ (green triangle). Solid line shows ground-state absorption spectrum of $P_{95}T_5$.

dynamics for intrachain energy transfer in the copolymers will be considered in more detail below.

Transient Absorption Spectroscopy. Nanosecond time-resolved transient absorption (TA) difference spectra were obtained on the series of homo- and copolymers to provide information regarding the nature of the $^3\pi,\pi^*$ states produced by photoexcitation. These experiments were conducted with 355 nm excitation, and the difference absorption spectra obtained immediately following the 10 ns laser excitation pulse are shown for comparison in Figure 5. All of the TA spectra are characterized by strong bleaching in the near-UV or blue region due to ground-state depletion, along with broad, moderately intense excited-state absorption extending throughout the visible region with a maximum between 600 and 650 nm. The visible absorption band is attributed to the $T_1 \rightarrow T_n$ absorption of the polymers.[8,40] This assignment is supported by the observation that there is good agreement between the TA and emission decay lifetimes (see Table 1 for the emission lifetime data).

Although the polymer TA spectra are qualitatively similar, there are quantitative differences between them that provide

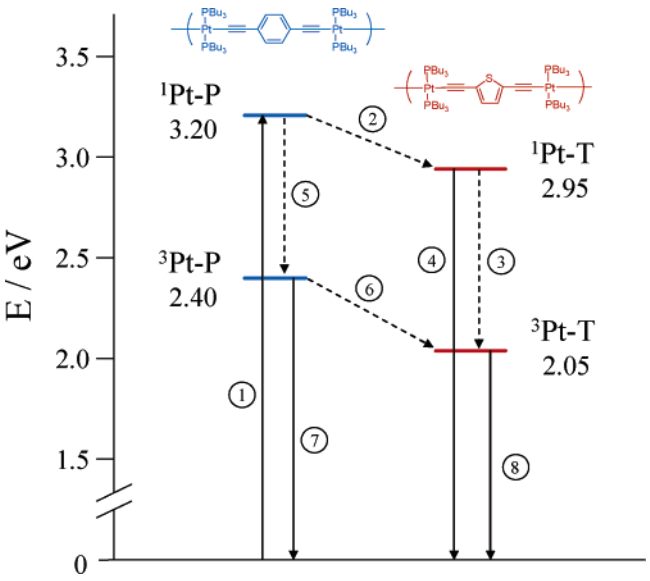

Figure 6. Jablonski diagram for copolymers.

information regarding the structure of the triplet states in the individual systems. In particular, by comparing the spectra in Figure 5a it can be seen that the most apparent difference in the TA of the homopolymers is the position of the ground-state bleach. In particular, the bleach is centered at ≈350 nm for P_{100} whereas it is shifted to ≈400 nm for T_{100}. The spectral shift in the TA bleach is consistent with the difference in the wavelength maxima for the ground-state absorption bands for the two polymers, as can be seen by comparison with the reference spectra shown in Figure 5a.

The TA spectra of the three copolymers are very similar (Figure 5b). All are dominated by a broad absorption with $\lambda_{max} \approx 610$ nm, accompanied by ground-state bleaching in the near-UV. The most interesting feature is the fact that the bleach for all three copolymers occurs at a wavelength corresponding closely to the ground-state absorption attributed to the Pt−T chromophore (ca. 395 nm). This is despite the fact that the absorption of the copolymers is dominated by the Pt−P chromophore which is at shorter wavelength (ca. 350 nm). The correspondence of the ground-state bleach with the low-energy chromophore is highlighted by comparison of the position of the ground-state bleach for $P_{95}T_5$ with the low energy (shoulder) in the ground-state absorption band of the same polymer (see reference spectrum in Figure 5b). The fact that the bleach in the TA spectra of the copolymers corresponds to the low-energy ground-state absorption band strongly implies that on the time scale of the nanosecond TA measurements the triplet is localized on a repeat unit that contains the (—Pt—C≡C—T—C≡C—Pt—) chromophore. The fact that the triplet is localized is consistent with the findings of previous work indicating that the triplet excited state in π-conjugated electronic systems is more localized compared to the singlet excited state.[9,39,44] In addition, the TA results indicate that at room temperature intrachain energy transfer as shown in eq 1 is complete on a time scale faster than is accessible with a nanosecond TA apparatus ($\tau <$ 10 ns, $k_{:} > 10^8$ s^{-1}). This fact is especially interesting for $P_{95}T_5$, where the 355 nm laser excitation predominately excites states localized on phenylene segments.

Mechanism of Intrachain Energy Transfer. The Jablonski diagram shown in Figure 6 provides information regarding the relative energies of the excited states for the Pt−acetylide copolymers, along with the pathways available for energy transfer and excited-state relaxation. The state energies are derived from the fluorescence and phosphorescence spectra of the homo- and copolymers.[45] The diagram is simplified to indicate states localized on Pt−P (left side) and Pt−T (right side) repeats; however, as discussed above, this is likely an oversimplification, especially for the relaxed $^1\pi,\pi^*$ state, which is likely delocalized over several Pt−acetylide units.[9] The states are labeled ^{1}Pt−P (or ^{3}Pt−P) and ^{1}Pt−T (or ^{3}Pt−T) to designate excitations localized on Pt-phenylene and Pt-thienylene chromophores, respectively. In the discussion below, it is assumed that photoexcitation initially creates a ^{1}Pt−P exciton. This assumption is reasonable, especially for the copolymer with the lowest loading of Pt−T units ($P_{95}T_5$), because in this case the near-UV absorption is dominated by the Pt−P chromophore.

There are two distinct mechanisms for intrachain energy transfer assuming that near-UV excitation of a copolymer initially produces a ^{1}Pt−P exciton (path 1, Figure 6). The first involves rapid singlet energy transfer from ^{1}Pt−P to afford ^{1}Pt−T (path 2, Figure 6). This process involves intrachain diffusion of the singlet exciton via Förster (dipole−dipole) or exchange hopping between proximal chromophores.[46] Following singlet transfer, ^{1}Pt−T can relax either radiatively (fluorescence) or via intersystem crossing to produce ^{3}Pt−T (paths 3 and 4, Figure 6). The second mechanism (triplet transfer) involves intersystem crossing on a Pt−P unit followed by intrachain triplet exciton transfer to a Pt−T unit (paths 5 and 6, Figure 6). The contribution of the two energy transfer paths depends strongly on the relative rates of intersystem crossing on the Pt−P unit and singlet transfer (paths 5 and 2, respectively). Previous work on Pt−acetylide oligomers indicates that intersystem crossing is fast ($\tau \approx 100$ ps, $k \approx 10^{10}$ s^{-1});[8] however, singlet transfer is also likely to be very rapid, especially when the loading of the Pt−T units in the chain is relatively high (e.g., in $Pt_{85}T_{15}$ and $Pt_{75}T_{25}$).

There is ample experimental evidence that both energy transfer mechanisms are active in the copolymers. First we consider the situation at room temperature. For $P_{85}T_{15}$ and $P_{75}T_{25}$, the singlet mechanism is believed to predominate. This notion is supported by the fact that for both polymers fluorescence from ^{1}Pt−T is observed (parts c and d of Figure 4), despite the fact that the excitation is absorbed largely by Pt−P units. The fact that singlet transfer predominates in these polymers is not surprising, given that the singlet state is relatively delocalized. Furthermore, due to the high loading of thienylenes in these copolymers, there is on average one Pt−T unit within every singlet chromophore (see Figure 3b). On the other hand, for $P_{95}T_5$ it is believed that at room temperature the triplet transfer pathway dominates. This conclusion is based on the fact that virtually no ^{1}Pt−T fluorescence is observed from this polymer, while the emission is dominated by the phosphorescence from ^{3}Pt−T.

The situation at low temperature (77 K) is distinctly different. In this case, for $P_{95}T_5$ and $P_{85}T_{15}$ there is little fluorescence observed from ^{1}Pt−T, and the total emission for both copolymers is dominated by phosphorescence from ^{3}Pt−P. This suggests that energy transfer by both the singlet and triplet paths is slowed significantly, and following initial excitation to ^{1}Pt−P, intersystem crossing to ^{3}Pt−P (path 5, Figure 6) is the predominant relaxation pathway. By contrast, even at 77 K the emission from $P_{75}T_{25}$ is dominated by phosphorescence from ^{3}Pt−T. This is likely a consequence of the high loading of the Pt−T units in the chain, making singlet transfer rapid even at low temperature.

Time-Resolved Emission Spectroscopy: Dynamics of Triplet Transfer. In an effort to obtain additional information

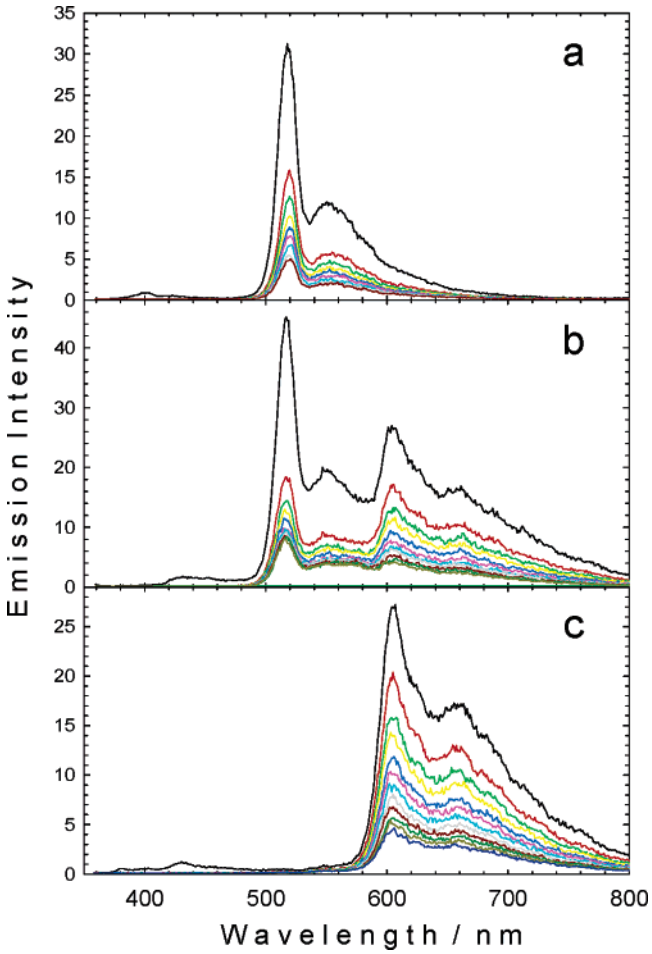

Figure 7. Time-resolved emission spectra obtained at 77 K for samples in argon degassed 2-MTHF following 355 nm excitation. Initial spectrum (most intense) was obtained with a 50 ns gate delay following excitation, and the succeeding spectra were obtained at 3 μs gate delay increments. Gate width 200 ns: (a) P_{100}, (b) $P_{95}T_5$, (c) T_{100}.

concerning the time scale of intrachain triplet exciton transport, time-resolved emission experiments were carried out on the homo- and copolymers.[47,48] These experiments were conducted using 10 ns pulsed laser excitation combined with a time gated/intensified CCD detector, which affords a time resolution of ca. 10 ns. Studies on the copolymers in THF solution at ambient temperature reveal that even at a 10 ns delay after excitation, the low-energy ^{3}Pt−T states dominate the emission. This result indicates that at ambient temperature intrachain energy transfer occurs on a time scale faster than is accessible with the instrumentation ($k > 10^8$ s^{-1}). Under these conditions, the long-lived emission from the copolymers is dominated by the ^{3}Pt−T phosphorescence which decays with lifetimes ranging from 5 to 10 μs (see Table 1).

Time-resolved emission experiments carried out with the copolymers in 2-MTHF at 77 K provide evidence that at low temperature the energy transfer dynamics are slowed significantly. In addition, even at very long times after excitation a fraction of the triplet excitons are trapped on high-energy Pt−P chromophores. In particular, Figure 7 compares time-resolved emission spectra obtained for P_{100}, $P_{95}T_5$, and T_{100} at 77 K. As can be seen in parts a and c of Figure 7, the emission from the homopolymers decays relatively uniformly over a 30 μs time scale. The time-resolved emission of the $P_{95}T_5$ copolymer is shown in Figure 7b for comparison. In this case it can be seen that the ^{3}Pt−P emission (515 nm) is approximately twice as intense as the ^{3}Pt−T emission (605 nm) at the earliest time delay; however, at longer delay times the intensity of the ^{3}Pt−P emission is comparable to that of the low-energy ^{3}Pt−T band. This suggests that at low temperature, there is a component of ^{3}Pt−P → ^{3}Pt−T energy transfer that occurs on a time scale of $\tau < 1$ μs ($k \approx 10^7$ s^{-1}); however, the existence of substantial ^{3}Pt−P emission at times longer than 1 μs after excitation suggests that a significant fraction of ^{3}Pt−P excitons are trapped and cannot undergo energy transfer on the microsecond time scale. It is possible that the "fast" relaxation of ^{3}Pt−P arises from excitations produced on a chain in close proximity to a Pt−T chromophore that are able to undergo energy transfer via a short-range hopping mechanism. By contrast, ^{3}Pt−P excitons that are produced some distance from a Pt−T trap may be unable to hop rapidly enough to compete with decay via radiative and nonradiative channels. Hopping may be slow because it involves energy transfer between "isoenergetic" chromophores (i.e., ^{3}Pt−P → ^{3}Pt−P, $\Delta G = 0$), and due to the lack of driving force the activation barrier is sufficiently large so as to preclude transfer at low temperature.

An important outcome of the steady-state and time-resolved work on the copolymers is that it provides evidence that intrachain triplet exciton transport in Pt−acetylides is a thermally activated process, and consequently, the dynamics are slowed significantly at low temperature. Although the origin of the activation barrier to triplet exciton transport is unknown, it is likely that intrachain triplet transfer occurs via a chromophore-to-chromophore hopping mechanism, and the individual steps have a reorganization energy that results from a difference in geometry between the ground and triplet excited states. Indeed in an ongoing experimental and theoretical study on Pt−acetylide oligomers, we have obtained solid evidence that the energetically preferred conformation of the aryl groups relative to the plane defined by the square-planar PtP_2C_2 units is different in the ground and triplet excited states.[49] Thus, the reorganization energy associated with intrachain triplet exciton hopping could be associated with the requirement for conformational rearrangement. Similar kinetic effects arising from large reorganization energies have been observed in studies of intramolecular electron and exchange energy transfer.[50−52]

Summary and Conclusions. A series of Pt−acetylide homo- and copolymers have been prepared and subjected to photophysical investigation to probe the mechanism and dynamics of intrachain triplet exciton migration. The copolymers feature 2,5-diethynylthienylene units doped into Pt−acetylide chains consisting predominantly of 1,4-diethynylphenylene repeats. The 2,5-diethynylthienylene moiety was selected as a low-energy "triplet" trap, on the basis of previous work which demonstrated that the $^3\pi,\pi^*$ state located on Pt−T units is ca. 0.35 eV lower in energy relative to that localized on Pt−P repeats.[4,38]

The absorption spectra of the copolymers are dominated by the π,π^* transition associated with the Pt−P repeat units; a shoulder at longer wavelengths is observed in $P_{95}T_5$ and $P_{85}T_{15}$ that is ascribed to chain segments containing Pt−T chromophores. The entire absorption band is red shifted in $P_{75}T_{25}$, which signals that in this polymer the loading of the Pt−T repeats in the polymer is sufficiently high such that there is on average one Pt−T repeat within every chromophore in the backbone. Steady-state and time-resolved photoluminescence and transient absorption spectroscopy studies of the copolymers demonstrate that at room temperature energy transfer to the Pt−T traps is rapid and efficient. Within 10 ns following laser excitation, the photoluminescence and transient absorption spectra are dominated by triplet states that are localized on Pt−T repeat units. The transient absorption spectra suggest that the

triplet state is relatively localized. By contrast, at 77 K photoluminescence spectroscopy indicates that energy transfer is considerably less efficient.

Energy transfer is believed to occur via two mechanisms. The first mechanism involves intrachain singlet transfer from an initially prepared ^{1}Pt−P state to produce ^{1}Pt−T, and after the exciton is localized on a Pt−T chromophore, intersystem crossing occurs to afford ^{3}Pt−T. This mechanism is believed to dominate for $P_{85}T_{15}$ and $P_{75}T_{25}$, which contains a relatively large fraction of Pt−T repeat units. The second mechanism involves ^{1}Pt−P → ^{3}Pt−P intersystem crossing followed by triplet energy transfer to produce ^{3}Pt−T. The available evidence suggests that this mechanism dominates in $P_{95}T_5$, where the loading of Pt−T units in the Pt−acetylide backbone is low.

Although the investigation does not provide quantitative information regarding the dyanamics of triplet exciton transport, the evidence is clear that at ambient temperature intrachain singlet and triplet energy transfer in Pt−acetylides is quite rapid. The fact that singlet transfer is rapid in the Pt−acetylides is consistent with the findings of previous investigations which demonstrate that intrachain singlet energy transfer is very fast in organic conjugated polymers.[23,35,46] On the other hand, as pointed out in the Introduction, relatively few studies have explored intrachain triplet exciton transport.[36] The results of the present investigation suggest that triplet transfer is rapid at ambient temperature, but the process appears to be accompanied by a moderate activation barrier. This barrier may be associated with low-frequency vibrational and rotational modes that are coupled to the ground-triplet excited-state transition.

Acknowledgment. We gratefully acknowledge the Air Force Office of Scientific Research (Grant No. F49620-03-1-0127) for support of this work.

References and Notes

(1) Skotheim, T. A.; Elsenbaumer, R. L.; Reynolds, J. R. *Handbook of Conducting Polymers*, 2nd ed.; Marcel Dekker: New York, 1998.

(2) McGehee, M. D.; Miller, E. K.; Moses, D.; Heeger, A. J. In *Advances in Synthetic Metals. Twenty Years of Progress in Science and Technology*; Bernier, P. L., S., Bidan, G., Eds.; Elsevier: Amsterdam, 1999; pp 98−205.

(3) Beljonne, D.; Wittmann, H. F.; Köhler, A.; Grahm, S. Y., M.; Lewis, J.; R., R. P.; Khan, M. S.; Friend, R. H.; Bredas, J. L. *J. Chem. Phys.* **1996**, *105*, 3868−3877.

(4) Chawdhury, N.; Köhler, A.; Friend, R. H.; Wong, W.-Y.; Lewis, J.; Younus, M.; Raithby, P. R.; Corcoran, T. C.; Al-Mandhary, M. R. A.; Khan, M. S. *J. Chem. Phys.* **1999**, *110*, 4963−4970.

(5) Kokil, A.; Shiyanovskaya, I.; Singer, K. D.; Weder, C. *J. Am. Chem. Soc.* **2002**, *124*, 9978−9979.

(6) Wilson, J. S.; Köhler, A.; Friend, R. H.; Al-Suti, M. K.; Al-Mandhary, M. R. A.; Khan, M. S.; Raithby, P. R. *J. Chem. Phys.* **2000**, *113*, 7627−7634.

(7) Wittmann, H. F.; Friend, R. H.; Khan, M. S.; Lewis, J. *J. Chem. Phys.* **1994**, *101*, 2693−2698.

(8) Rogers, J. E.; Cooper, T. M.; Fleitz, P. A.; Glass, D. J.; McLean, D. G. *J. Phys. Chem. A* **2002**, *106*, 10108−10115.

(9) Liu, Y.; Jiang, S.; Glusac, K.; Powell, D. H.; Anderson, D. F.; Schanze, K. S. *J. Am. Chem. Soc.* **2002**, *124*, 12412−12413.

(10) Wilson, J. S.; Dhoot, A. S.; Seeley, A. J. A. B.; Khan, M. S.; Köhler, A.; Friend, R. H. *Nature* **2001**, *413*, 828−831.

(11) Baldo, M. A.; O'Brien, D. F.; You, Y.; Shoustikov, A.; Sibley, S.; Thompson, M. E.; Forrest, S. R. *Nature* **1998**, *395*, 151−154.

(12) Staromlynska, J.; McKay, T. J.; Bolger, J. A.; Davy, J. R. *J. Opt. Soc. Am. B* **1998**, *12*, 1731−1736.

(13) Babel, A.; Jenekhe, S. A. *J. Phys. Chem. B* **2003**, *107*, 1749−1754.

(14) Campbell, I. H.; Smith, D. L.; Neef, C. J.; Ferraris, J. P. *Appl. Phys. Lett.* **1999**, *74*, 2809−2811.

(15) Sirringhaus, H.; Tessler, N.; Friend, R. H. *Science* **1998**, *280*, 1741−1744.

(16) Bredas, J. L.; Beljonne, D.; Coropceanu, V.; Cornil, J. *Chem. Rev.* **2004**, *104*, 4971−5003.

(17) Harrison, B. S.; Foley, T. J.; Knefely, A. S.; Mwaura, J. K.; Cunningham, G. B.; Kang, T. S.; Bouguettaya, M.; Boncella, J. M.; Reynolds, J. R.; Schanze, K. S. *Chem. Mater.* **2004**, *16*, 2938−2947.

(18) Brunner, K.; van Haare, J. A. E. H.; Langeveld-Voss, B. M. W.; Schoo, H. F. M.; Hofstraat, J. W.; van Dijken, A. *J. Phys. Chem. B* **2002**, *106*, 6834−6841.

(19) Kim, J. S.; McQuade, D. T.; Rose, A.; Zhu, Z. G.; Swager, T. M. *J. Am. Chem. Soc.* **2001**, *123*, 11488−11489.

(20) Levitsky, I. A.; Kim, J. S.; Swager, T. M. *J. Am. Chem. Soc.* **1999**, *121*, 1466−1472.

(21) Kim, J.; Levitsky, I. A.; McQuade, D. T.; Swager, T. M. *J. Am. Chem. Soc.* **2002**, *124*, 7710−7718.

(22) Bumm, L. A.; Arnold, J. J.; Cygan, M. T.; Dunbar, T. D.; Burgin, T. P.; Jones, L.; Allara, D. L.; Tour, J. M.; Weiss, P. S. *Science* **1996**, *271*, 1705−1707.

(23) Swager, T. M.; Gil, C. J.; Wrighton, M. S. *J. Phys. Chem.* **1995**, *99*, 4886−4893.

(24) Swager, T. M. *Acc. Chem. Res.* **1998**, *31*, 201−207.

(25) Chen, L.; McBranch, D. W.; Wang, H.-L.; Helgeson, R.; Wudl, F.; Whiten, D. G. *Proc. Natl. Acad. Sci. U.S.A.* **1999**, *96*, 12287−12292.

(26) Harrison, B. S.; Ramey, M. B.; Reynolds, J. R.; Schanze, K. S. *J. Am. Chem. Soc.* **2000**, *122*, 8561−8562.

(27) Wang, J.; Wang, D. L.; Miller, E. K.; Moses, D.; Bazan, G. C.; Heeger, A. J. *Macromolecules* **2000**, *33*, 5153−5158.

(28) Tan, C.; Pinto, M. R.; Schanze, K. S. *Chem. Commun.* **2002**, 446−447.

(29) Wang, B.; Wasielewski, M. R. *J. Am. Chem. Soc.* **2002**, *119*, 12−21.

(30) Lui, Y.; Jiang, S.; Schanze, K. S. *Chem. Commun.* **2003**, 650−651.

(31) Funston, A. M.; Silverman, E. E.; Miller, J. R.; Schanze, K. S. *J. Phys. Chem. B* **2004**, *108*, 1544−1555.

(32) Candeias, L. P.; Grozema, F. C.; Padmanaban, G.; Ramakrishnan, S.; Siebbeles, L. D. A.; Warman, J. M. *J. Phys. Chem. B* **2003**, *107*, 1554−1558.

(33) Zhou, Q.; Swager, T. M. *J. Am. Chem. Soc.* **1995**, *117*, 12593−12602.

(34) Chen, L.; McBranch, D. W.; Wang, H.-L.; Helgeson, R.; Wudl, F.; Whitten, D. G. *Proc. Natl. Acad. Sci. U.S.A.* **1999**, *96*, 12287−12292.

(35) Tan, C.; Atas, E.; Müller, J. G.; Pinto, M. R.; Kleiman, V. D.; Schanze, K. S. *J. Am. Chem. Soc.* **2004**, *126*, 13685−13694.

(36) Haskins-Glusac, K.; Pinto, M. R.; Tan, C.; Schanze, K. S. *J. Am. Chem. Soc.* **2004**, *126*, 14964−14971.

(37) Takahashi, S.; Kuroyama, Y.; Sonogashira, K.; Hagihara, N. *Synthesis* **1980**, 627−630.

(38) Wilson, J. S.; Chawdhury, N.; Al-Mandhary, M. R. A.; Younus, M.; Khan, M. S.; Raithby, P. R.; Köhler, A.; Friend, R. H. *J. Am. Chem. Soc.* **2001**, *123*, 9412−9417.

(39) Köhler, A.; Wilson, J. S.; Friend, R. H.; Al-Suti, M. K.; Khan, M. S.; Gerhard, A.; Bassler, H. *J. Chem. Phys.* **2002**, *116*, 9457−9463.

(40) Zhao, X.; Cardolaccia, T.; Farley, R. T.; Abboud, K. A.; Schanze, K. S. *Inorg. Chem.* **2005**, *44*, 2619−2627.

(41) Harriman, A. *Chem. Commun.* **1997**, 7777−7778.

(42) Demas, J. N.; Crsoby, G. A. *J. Phys. Chem.* **1971**, *75*, 995−1024.

(43) Wang, Y. S.; Schanze, K. S. *Chem. Phys.* **1993**, *176*, 305−319.

(44) Beljonne, D.; Wittmann, H. F.; Köhler, A.; Graham, S.; Younus, M.; Lewis, J.; Raithby, P. R.; Khan, M. S.; Friend, R. H.; Bredas, J. L. *J. Chem. Phys.* **1996**, *105*, 3868−3877.

(45) The fluorescence energy for the Pt-phenylene chromophore is taken from a previous investigation of Pt-acetylide oligomers; see ref 9.

(46) Beljonne, D.; Pourtois, G.; Silva, C.; Hennebicq, E.; Herz, L. M.; Friend, R. H.; Scholes, G. D.; Setayesh, S.; Mullen, K.; Bredas, J. L. *Proc. Natl. Acad. Sci. U.S.A.* **2002**, *99*, 10982−10987.

(47) A more detailed description of the time-resolved emission experiments and results is available in Eric Silverman's Ph.D. dissertation; see ref 48.

(48) Silverman, E. E. Photophysics of Single Chain Poly(Arylene Ethynylene)s. Ph.D. Dissertation, University of Florida, Gainesville, FL, 2005, http://chem.ufl.edu/~kschanze/thesis/silverman.pdf.

(49) Haskins-Glusac, K. Photophysics of Platinum-Acetylides. Ph.D. Dissertation, University of Florida, Gainesville, FL, 2003, http://www.chem.ufl.edu/~kschanze/thesis/glusac.pdf.

(50) Miller, J. R.; Pavlatos, B.; Bal, R.; Closs, G. L. *J. Phys. Chem.* **1995**, *99*, 6923−6925.

(51) Sigman, M. E.; Closs, G. L. *J. Phys. Chem.* **1991**, *95*, 5012−5017.

(52) Zhang, D.; Closs, G. L.; Chung, D. D.; Norris, J. R. *J. Am. Chem. Soc.* **1993**, *115*, 3670−3673.